Journal of Materials Chemistry A

COMMUNICATION

View Article Online
View Journal

Cite this: DOI: 10.1039/c5ta01434d

Received 24th February 2015
Accepted 14th April 2015

DOI: 10.1039/c5ta01434d

www.rsc.org/MaterialsA

AgPd@Pd/TiO_2 nanocatalyst synthesis by microwave heating in aqueous solution for efficient hydrogen production from formic acid†

Masashi Hattori,[a] Daisuke Shimamoto,[b] Hiroki Ago[a] and Masaharu Tsuji*[a]

$Ag_{100-x}Pd_x/TiO_2$ ($x = 7$, 10, and 15) catalysts for hydrogen production from formic acid were synthesized in aqueous solution using MW heating. The hydrogen production rate of $Ag_{100-x}Pd_x$@Pd/TiO_2 increased concomitantly with decreasing x. The best catalytic activity ever reported was obtained for $Ag_{93}Pd_7$@Pd/TiO_2 among all heterogeneous catalysts.

The search for effective techniques of hydrogen gas (H_2) generation from liquid fuels has remained a difficult challenge for mobile hydrogen energy systems. Formic acid (FA) attracts great attention as a liquid fuel because of its high energy density, nontoxicity, and excellent stability at room temperature. Moreover, FA is producible by a combination of H_2O and CO_2 by irradiation with sunlight as a primary product in artificial photosynthesis,[1–3] which makes FA more attractive for use in a sustainable and reversible energy storage cycle.

Some reports have described hydrogen production from the decomposition of formic acid using solid catalysts such as core–shell Au@Pd/C catalysts.[4,5] Shortcomings of most such catalysts are high operating temperature (>80 °C) for efficient FA decomposition and reduction of catalytic activity because of CO coproduction. These shortcomings were overcome using an Ag@Pd core–shell nanocatalyst, for which a high initial hydrogen rate of about 4 L g^{-1} h^{-1} was achieved at room temperature without CO coproduction.[6] The high catalytic activity of Ag@Pd core–shell nanocatalysts was explained by electron transfer from the Ag core to the Pd shell because of the larger work function of Pd (5.1 eV) than that of Ag (4.7 eV).[6]

We recently studied the preparation of Ag@Pd nanocatalysts loaded on TiO_2 nanoparticles using a two-step microwave-polyol method, where ethylene glycol (EG) was used as both a solvent and a reductant. In the first step, small Ag core particles were prepared in the presence of TiO_2 particles. Then Pd shells were synthesized in the second step. Based on spherical-aberration-corrected scanning transmission electron microscopy (STEM), STEM-energy dispersed X-ray spectroscopy (EDS), X-ray diffraction (XRD), and X-ray photoelectron spectroscopy (XPS) data, we demonstrated the preparation of Ag–Pd alloy core and Pd shell nanocrystals loaded on anatase-type of TiO_2 nanoparticles (denoted as AgPd@Pd/TiO_2). Ag and Pd atoms are partially alloyed with each other under heating above 170 °C. Therefore, $Ag_{82}Pd_{18}$ alloy and Pd shell nanocatalysts were formed. Using TiO_2 support, a higher hydrogen production rate of 16.00 ± 0.89 L g^{-1} h^{-1} than that in the previous report[6] was obtained. When we compared the effects of TiO_2 support using AgPd@Pd catalysts without TiO_2 support (denoted as bare AgPd@Pd), the initial hydrogen production rate of AgPd@Pd/TiO_2 was 23 times higher than that of bare AgPd@Pd. Significant enhancement of catalytic activity of AgPd@Pd in the presence of TiO_2 was explained by further electron transfer from TiO_2 to Pd because the work function of TiO_2 (4.0 eV) is lower than that of Pd (5.1 eV).[7]

For the practical application of AgPd@Pd/TiO_2 catalysts, even higher activity is required. Based on previous work on catalytic activity of the Ag–Pd bimetallic system,[6] the catalytic activity of the AgPd alloy catalyst was much lower than that of core–shell catalysts. These facts suggest that the catalytic activity of Ag@Pd core–shell catalysts decreases greatly by alloying between the Ag core and the Pd shell. Consequently, it is expected that the catalytic activity of AgPd@Pd/TiO_2 can be greatly enhanced by dealloying the AgPd core. For this purpose, a new simple method for preparing AgPd@Pd/TiO_2 catalysts with a low Pd content in the AgPd core must be developed.

In our previous study, AgPd@Pd/TiO_2 catalysts were synthesized in EG by MW heating at 176–178 °C for about 10 min.[7] The Ag core and Pd shell were partially alloyed under heating at such a high temperature. This communication describes our attempt to prepare AgPd@Pd/TiO_2 catalysts having a lower Pd content in AgPd at much lower temperature under MW heating. Here we use an aqueous solution as the solvent. The reagent solution was

[a]Institute for Materials Chemistry and Engineering, Kyushu University, Kasuga 816-8580, Japan. E-mail: tsuji@cm.kyushu-u.ac.jp

[b]Department of Applied Science for Electronics and Materials, Graduate School of Engineering Sciences, Kyushu University, Kasuga 816-8580, Japan

† Electronic supplementary information (ESI) available. See DOI: 10.1039/c5ta01434d

kept at about 100 °C. The effect of alloying in the AgPd core on the catalytic activity was examined by changing the heating time used for the preparation of AgPd@Pd/TiO_2 catalysts. Results show that catalytic activity depends strongly on the extent of alloying of the AgPd core. We have succeeded in the preparation of $Ag_{100-x}Pd_x$@Pd/TiO_2 ($x = 7$, 10, and 15) catalysts having much higher catalytic activity than that of $Ag_{82}Pd_{18}$@Pd/TiO_2 catalysts obtained in EG.[7]

AgPd@Pd/TiO_2 was prepared using the following method. First, Ag core nanoparticles were formed in the presence of anatase-type of TiO_2 nanoparticles with 10 nm average diameter, synthesized by MW heating[8] (see STEM and XRD data in Fig. S1, ESI†). Then 15 mL of distilled water containing 300 mg polyvinylpyrrolidone (PVP) and 12.26 mg $AgNO_3$ was mixed with the colloidal solution of 71.88 mg TiO_2 nanoparticles. The mixed solution was heated at 95 °C with MW irradiation at 120 W for 40 min under Ar bubbling. In the second step, 2 mL of distilled water containing 8.3 mg $Pd(NO_3)_2$ was added to this solution and heated with MW irradiation at 400 W for 30 min, 1 h, or 2 h under Ar bubbling. Typical temperature profiles of MW heating when Ag nanoparticles and Pd shell were formed are shown in Fig. S2 (ESI†). These products are respectively called AgPd@Pd/TiO_2 (30 min), AgPd@Pd/TiO_2 (1 h), and AgPd@Pd/TiO_2 (2 h) hereinafter. The solution temperature increased to about 100 °C under MW irradiation. Characterization of product particles was conducted using STEM, STEM–EDS, XRD, XPS, and atomic absorption spectrometry (AAS). The hydrogen production rate was determined using a gas burette. Further details related to experimental methods are described in the ESI.† Fig. S3 (ESI†) shows a typical STEM image of TiO_2 and Ag particles, where some strong white contrast Ag particles are not loaded on light contrast TiO_2 particles.

Fig. 1a–e show STEM and STEM-EDS images of AgPd@Pd/TiO_2 (30 min). Fig. 1f shows line analysis data along the red line depicted in Fig. 1d. Results show that Ag–Pd bimetallic nanocatalysts with an average diameter of 4.6 ± 0.9 nm were loaded uniformly on TiO_2 nanoparticles and an approximately 0.8 nm-thick pure Pd shell was formed on the Ag or the Ag–Pd alloy core metal. The Pd/Ag atomic ratio in whole Ag–Pd bimetallic nanocatalysts was determined to be 0.32 ± 0.02 using STEM-EDS analysis. The Pd/Ag atomic ratio was also analyzed using AAS (see ESI†). The result obtained was in reasonable agreement with that estimated from the STEM-EDS analysis. STEM and STEM-EDS images of AgPd@Pd/TiO_2 (1 h) and AgPd@Pd/TiO_2 (2 h) were also observed (see Fig. S4 and S5, ESI†). These results show that AgPd@Pd nanocatalysts of AgPd@Pd/TiO_2 (1 h) and AgPd@Pd/TiO_2 (2 h) respectively had an average diameter of 4.4 ± 0.7 nm and 4.5 ± 1.1 nm and about 0.6 nm-thick and 0.5 nm-thick pure Pd shell. The Pd/Ag atomic ratio in whole AgPd@Pd nanocatalysts of AgPd@Pd/TiO_2 (1 h) and AgPd@Pd/TiO_2 (2 h) was determined to be 0.33 ± 0.03 and 0.31 ± 0.01 from STEM-EDS analysis. These results show that all samples had nearly the same morphology, size, and composition, which indicates that added $Pd(NO_3)_2$ was reduced completely and that AgPd@Pd nanoparticles were formed by MW heating in 30 min.

Fig. 2 shows XRD patterns of AgPd@Pd/TiO_2 (30 min), AgPd@Pd/TiO_2 (1 h), and AgPd@Pd/TiO_2 (2 h) in the 2θ = 20–90° range. An expanded XRD pattern in the 2θ = 37–40° range is shown in Fig. S6 (ESI†), where a major peak of the Ag component is observed. Aside from TiO_2 anatase-peaks observed at 2θ = 25.2°, 47.9°, 53.5°, 54.9°, and 62.4° indexed to {101}, {200}, {105}, {211} and {204} facets (PDF 01-071-1168), major peaks derived from {111}, {200}, {220}, and {311} facets of the Ag component of fcc Ag–Pd bimetallic particles were observed. However, these peaks slightly shift to larger 2θ from those of pure fcc Ag crystals (PDF 01-071-3762: 2θ = 38.12°, 44.31°, 64.45°, and 77.41° for {111}, {200}, {220}, and {311}, respectively). These peak shifts occur by alloying of the Ag core and Pd. According to Vegard's law,[9] which is known to be

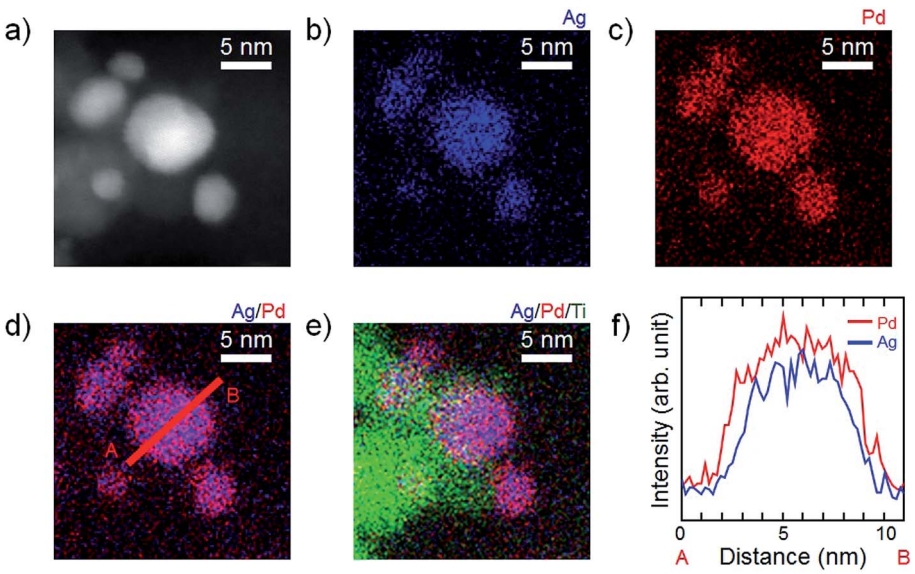

Fig. 1 STEM and STEM-EDS images of the AgPd@Pd/TiO_2 (30 min) nanocatalysts: (a) STEM image, (b) Ag component, (c) Pd component, (d) Ag and Pd components, (e) all components, and (f) line analysis data along the red line shown in panel (e).

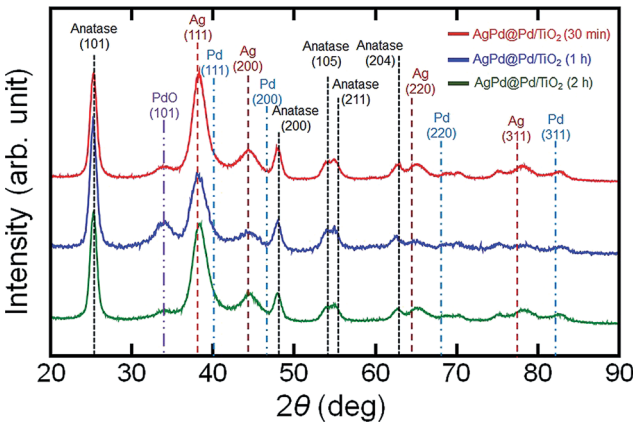

Fig. 2 XRD patterns of all AgPd@Pd/TiO_2 nanocatalysts.

applicable to Ag–Pd systems,[10] about 7.4%, 10.1%, and 15.3% of Pd atoms are dissolved respectively in AgPd alloy core particles of AgPd@Pd/TiO_2 (30 min), AgPd@Pd/TiO_2 (1 h), and AgPd@Pd/TiO_2 (2 h). Here, a weak peak was observed at $2\theta = 34.4°$ in all samples indexed to {101} facets of PdO (PDF 01-088-2434), which was not observed in Ag–Pd particles of AgPd@Pd/TiO_2 prepared in EG solution (denoted as AgPd@Pd/TiO_2 (EG)).[7] This result means that a small amount of PdO was formed under MW heating in aqueous solution. Moreover, the fact that the intensity ratio of the PdO {101} peak to the Ag {111} peak was

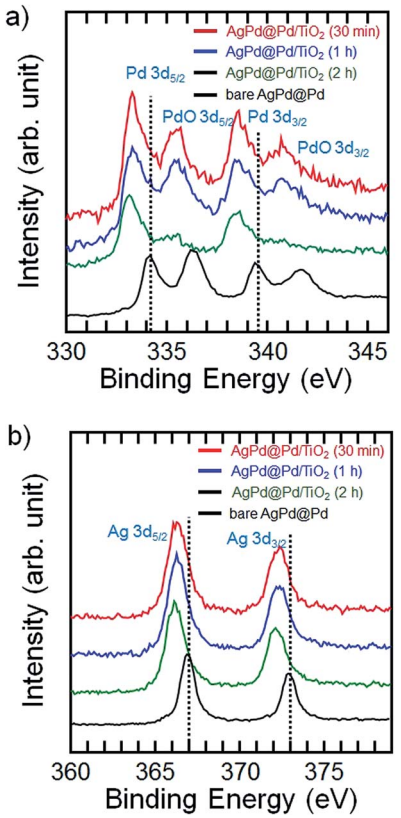

Fig. 3 XPS spectra of all AgPd@Pd/TiO_2 nanocatalysts and bare AgPd@Pd nanocatalyst: (a) Pd $3d_{3/2,5/2}$ and (b) Ag $3d_{3/2,5/2}$.

AgPd@Pd/TiO_2 (1 h) > AgPd@Pd/TiO_2 (30 min) ≈ AgPd@Pd/TiO_2 (2 h), indicating that the relative amount of PdO to Ag is independent of the reaction time.

To characterize the chemical states of AgPd@Pd/TiO_2 samples, XPS spectra were measured (Fig. 3a and b). For comparison, bare AgPd@Pd nanoparticles prepared using the same process as that of AgPd@Pd/TiO_2 (30 min) were also measured. In the XPS spectra of the 330–346 eV range (Fig. 3a), Pd 3d and PdO 3d peaks were observed in all samples. The intensity ratio of the PdO peak to the Pd peak is independent of the reaction time. These results also show that PdO was formed under MW heating in aqueous solution and the amount of PdO was not correlated with the reaction time. The Pd $3d_{5/2}$ and $3d_{3/2}$ peaks in bare AgPd@Pd shift to lower values by about 1.0 eV compared to those of pure Pd ($3d_{5/2}$ = 335.1 eV, $3d_{5/2}$ = 340.3 eV) because of electron transfer from Ag to Pd arising from a difference of work functions between Ag and Pd. Similarly, the binding energies of Ag $3d_{5/2}$ and $3d_{3/2}$ peaks in bare AgPd@Pd shift to lower values by about 1.2 eV compared with those of pure Ag 3d ($3d_{5/2}$ = 368.2 eV, $3d_{3/2}$ = 374.2 eV). These binding energies were similar to those of Ag 3d peaks in Pd rich (>90%) Ag–Pd alloys.[11] Therefore, it is reasonable to assume that the peak shifts originate from the formation of Ag–Pd alloys around the interface of the Ag-core and the Pd-shell.

The binding energies of Pd $3d_{5/2}$ and $3d_{3/2}$ peaks of all three AgPd@Pd/TiO_2 samples were almost identical and shifted to lower values by about 0.9 eV compared to those of bare AgPd@Pd nanoparticles ($3d_{5/2}$ = 334.2 eV, $3d_{3/2}$ = 339.4 eV). At the same time, the binding energies for Ag $3d_{5/2}$ and $3d_{3/2}$ peaks of all AgPd@Pd/TiO_2 samples were also almost identical and shifted to lower values by about 0.9 eV compared with those of bare AgPd@Pd nanoparticles ($3d_{5/2}$ = 367.1 eV, $3d_{3/2}$ = 373.0 eV). These shifts suggest that some electrons are transferred from TiO_2 to Pd and Ag because of large differences of the work functions between Ag or Pd and TiO_2. Taking account of the fact that the binding energies for Ag and Pd are almost identical in all $Ag_{100-x}Pd_x$@Pd/TiO_2 (x = 7, 10, and 15) samples, AgPd@Pd nanoparticles were sufficiently adhered onto TiO_2 by MW heating for 30 min.

The initial H_2 production rate ($R_{hydrogen}$) of AgPd@Pd/TiO_2 samples was measured using the following method: total gas volume from a stirred glass tube containing 20 mL of 0.25 M aqueous formic acid and the prepared sample (metallic catalyst weight of 5.1 mg) was measured using a gas burette (see Fig. S7, ESI†). Detailed gas analyses for CO_2, H_2, and CO were performed on a gas chromatograph and no CO emission was detected using GC for all samples at 27–90 °C (see Fig. S8, ESI†). Temporal variation of total gas generation by decomposition of formic acid in the presence of $Ag_{93}Pd_7$@Pd/TiO_2 (30 min), $Ag_{90}Pd_{10}$@Pd/TiO_2 (1 h), and $Ag_{85}Pd_{15}$@Pd/TiO_2 (2 h) at room temperature (27 °C) is shown in Fig. 4a. The $R_{hydrogen}$ values obtained from eqn (S1) and (S2) of ESI† are presented in Table 1. For comparison, the corresponding data for $Ag_{82}Pd_{18}$@Pd/TiO_2,[7] bare Ag@Pd,[6] and CoAuPd alloy nanoparticles[12] are given. The $R_{hydrogen}$ value of the $Ag_{93}Pd_7$@Pd/TiO_2 (30 min) sample increases greatly from 46.03 L g^{-1} h^{-1} at 27 °C to 371.79 L g^{-1} h^{-1} at 90 °C. The $R_{hydrogen}$ value at 27 °C is about three times

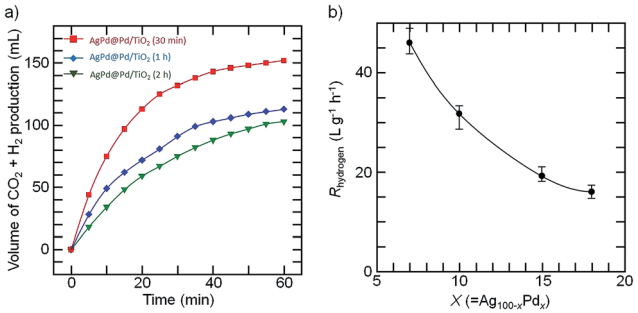

Fig. 4 (a) Gas generation by decomposition of formic acid (0.25 M, 20 mL) *vs.* time in the presence of AgPd@Pd/TiO_2 (30 min) nanocatalysts, AgPd@Pd/TiO_2 (1 h) nanocatalysts and AgPd@Pd/TiO_2 (2 h) nanocatalysts at 27 °C. (b) The hydrogen generation rate variation of AgPd@Pd/TiO_2 samples follows the alloying rate of $Ag_{100-x}Pd_x$ at 27 °C.

Table 1 Hydrogen production rates from catalytic decomposition of formic acid in water at different temperatures

Catalyst	Temperature (°C)	H_2 gas volume (L g^{-1} h^{-1})
$Ag_{93}Pd_7$@Pd/TiO_2 (30 min)	27	46.03 ± 2.27
$Ag_{93}Pd_7$@Pd/TiO_2 (30 min)	40	91.06 ± 4.80
$Ag_{93}Pd_7$@Pd/TiO_2 (30 min)	60	143.77 ± 3.33
$Ag_{93}Pd_7$@Pd/TiO_2 (30 min)	70	230.40 ± 5.69
$Ag_{93}Pd_7$@Pd/TiO_2 (30 min)	90	371.79 ± 9.86
$Ag_{90}Pd_{10}$@Pd/TiO_2 (1 h)	27	31.74 ± 1.64
$Ag_{90}Pd_{10}$@Pd/TiO_2 (1 h)	40	57.96 ± 3.08
$Ag_{90}Pd_{10}$@Pd/TiO_2 (1 h)	60	128.52 ± 5.85
$Ag_{90}Pd_{10}$@Pd/TiO_2 (1 h)	70	149.06 ± 6.38
$Ag_{90}Pd_{10}$@Pd/TiO_2 (1 h)	90	285.04 ± 12.01
$Ag_{85}Pd_{15}$@Pd/TiO_2 (2 h)	27	19.17 ± 1.49
$Ag_{85}Pd_{15}$@Pd/TiO_2 (2 h)	40	33.68 ± 0.32
$Ag_{85}Pd_{15}$@Pd/TiO_2 (2 h)	60	75.85 ± 1.32
$Ag_{85}Pd_{15}$@Pd/TiO_2 (2 h)	70	128.05 ± 8.22
$Ag_{85}Pd_{15}$@Pd/TiO_2 (2 h)	90	253.21 ± 10.54
$Ag_{82}Pd_{18}$@Pd/TiO_2 (EG)[7]	27	16.00 ± 0.89
Ag@Pd[6]	20	3.67
CoAuPd[12]	25	7.9

higher than that of $Ag_{82}Pd_{18}$@Pd/TiO_2 (EG) at 27 °C (16.00 L g^{-1} h^{-1})[7] and about 13 and 6 times higher than those of Ag@Pd catalysts at 20 °C (3.67 L g^{-1} h^{-1})[6] and CoAuPd alloy catalysts at 25 °C (7.9 L g^{-1} h^{-1}).[12] On the other hand, the $R_{hydrogen}$ values of $Ag_{90}Pd_{10}$@Pd/TiO_2 (1 h) and $Ag_{85}Pd_{15}$@Pd/TiO_2 (2 h) samples were, respectively, 31.74 L g^{-1} h^{-1} and 19.17 L g^{-1} h^{-1} at 27 °C. Fig. 4b shows the dependence of $R_{hydrogen}$ on Pd contents in the AgPd core. It is noteworthy that the $R_{hydrogen}$ value increases greatly with decreasing Pd content in the AgPd core and that the catalytic activity is independent of the amount of PbO which was largest in AgPd@Pd/TiO_2 (1 h). These results indicate that the catalytic activity depends on the extent of alloying between Ag and Pd in the AgPd core under our experimental conditions.

Hydrogen gas production rates were measured at various temperatures using AgPd@Pd/TiO_2 catalysts (Table 1). The apparent activation energies were estimated from the following relationship.

$$\ln(R_{hydrogen}) = -E_a/RT + C \quad (1)$$

In this equation, $R_{hydrogen}$ is the initial rate of hydrogen generation, E_a is the apparent activation energy, and C is a constant. The E_a values were estimated respectively to be 29.8, 32.5, and 37.8 kJ mol^{-1} for $Ag_{93}Pd_7$@Pd/TiO_2 (30 min), $Ag_{90}Pd_{10}$@Pd/TiO_2 (1 h), and $Ag_{85}Pd_{15}$@Pd/TiO_2 (2 h) (see Fig. S9, ESI†). These values were higher than E_a of $Ag_{82}Pd_{18}$@Pd/TiO_2 prepared in EG solution (7.2 kJ mol^{-1}).[7] The formation of PdO on the surface, which interferes with the catalytic activity, might be one reason for the increase in E_a values.

In the last section we discuss on the origin of decrease in the catalytic activity with increasing x in $Ag_{100-x}Pd_x$@Pd/TiO_2 nanocatalysts. The atomic ratios of the Pd shell to the AgPd core in $Ag_{100-x}Pd_x$(x = 7, 10, and 15)@Pd particles were estimated from STEM-EDS and XRD data to be 0.25, 0.21 and 0.15, respectively. This result suggests that the Pd/AgPd atomic ratio decreases with an increasing x. On the other hand, we found that the total Pd/Ag atomic ratio of $Ag_{100-x}Pd_x$@Pd/TiO_2 was nearly constant between 30 min and 2 h of heating. In addition, the particle sizes of $Ag_{100-x}Pd_x$@Pd of all samples were almost the same (≈4.6 nm). On the basis of the above findings, reduction of Pd^{2+} on the Ag or AgPd core is completed within 30 min and alloying between the Ag core and the Pd shell occurs between 30 min and 2 h. Tsang *et al.*[6] reported that Ag@Pd nanocatalysts showed their highest catalytic activity when the Ag core was completely covered by a thin Pd shell. The catalytic activity rapidly dropped off both when the surface area of the Pd shell became low or the Pd shell became thicker. It is therefore reasonable to assume that the surface area of the Pd shell of $Ag_{100-x}Pd_x$@Pd nanoparticles prepared in this study decreases with an increasing x because Pd atoms in the Pd shell decrease owing to alloying between the Ag core and the Pd shell at longer MW heating.

Conclusions

For this study, we prepared $Ag_{100-x}Pd_x$@Pd/TiO_2 (x = 7, 10, and 15) nanocatalysts under MW heating in aqueous solution for suppressing the alloying of the Ag core and Pd. The hydrogen generation rates of $Ag_{100-x}Pd_x$@Pd/TiO_2 (x = 7, 10, and 15) catalysts depend strongly on the degree of alloying in $Ag_{100-x}Pd_x$@Pd/TiO_2 catalysts. They increase by 2.4 times with a decrease in the Pd content in the AgPd core from 15% to 7%. The initial hydrogen formation rate of $Ag_{93}Pd_7$@Pd/TiO_2 (30 min) from formic acid, 46.03 L g^{-1} h^{-1}, was about three times higher than that of $Ag_{82}Pd_{18}$@Pd/TiO_2 (EG).[7] To the best of our knowledge, this is the best value ever reported among all heterogeneous catalysts.[6,12] Our novel method for producing high catalytic activity of core–shell AgPd@Pd nanocatalysts on TiO_2 particles under low temperature conditions is applicable for efficient hydrogen production systems intended for mobile applications.

Acknowledgements

This work was supported by JSPS KAKENHI Grant numbers 25286003 and 25550056, and by a Management Expenses Grant for National University Corporations from MEXT.

Notes and references

1 S. Sato, T. Arai, T. Morikawa, K. Uemura, T. M. Suzuki, H. Tanaka and T. Kajino, *J. Am. Chem. Soc.*, 2011, **133**, 15240–15243.
2 M. Mikkelsen, S. Sato, T. Kajino and T. Morikawa, *Energy Environ. Sci.*, 2010, **3**, 43–81.
3 T. Arai, M. Jorgensen and F. C. Krebs, *Energy Environ. Sci.*, 2013, **6**, 1274–1282.
4 X. C. Zhou, Y. Huang, W. Xing, C. Liu, J. Liao and T. Lu, *Chem. Commun.*, 2008, 3540–3542.
5 Y. Huang, X. Zhou, M. Yin, C. Liu and W. Xing, *Chem. Mater.*, 2010, **22**, 5122–5128.
6 K. Tedsree, T. Li, S. Jones, C. W. A. Chan, K. M. K. Yu, P. A. J. Bagot, E. A. Marquis, G. D. W. Smith and S. C. E. Tsang, *Nat. Nanotechnol.*, 2011, **6**, 302–307.
7 M. Hattori, H. Einaga, T. Daio and M. Tsuji, *J. Mater. Chem. A*, 2015, **3**, 4453–4461.
8 T. Yamamoto, Y. Wada, H. Yin, T. Sakata, H. Mori and S. Yanagida, *Chem. Lett.*, 2011, **38**, 964–965.
9 A. R. Denton and N. W. Ashcroft, *Phys. Rev. A*, 1991, **43**, 3161–3164.
10 L. Chen and Y. Liu, *J. Colloid Interface Sci.*, 2011, **364**, 100–106.
11 P. Steiner and S. Hufner, *Solid State Commun.*, 1981, **37**, 79–81.
12 Z.-L. Wang, J.-M. Yan, Y. Ping, H.-L. Wang, W.-T. Zheng and Q. Jiang, *Angew. Chem., Int. Ed.*, 2013, **52**, 4406–4409.